Di-Higgs Physics at Future Circular Colliders

Ashutosh Kotwal
Duke University

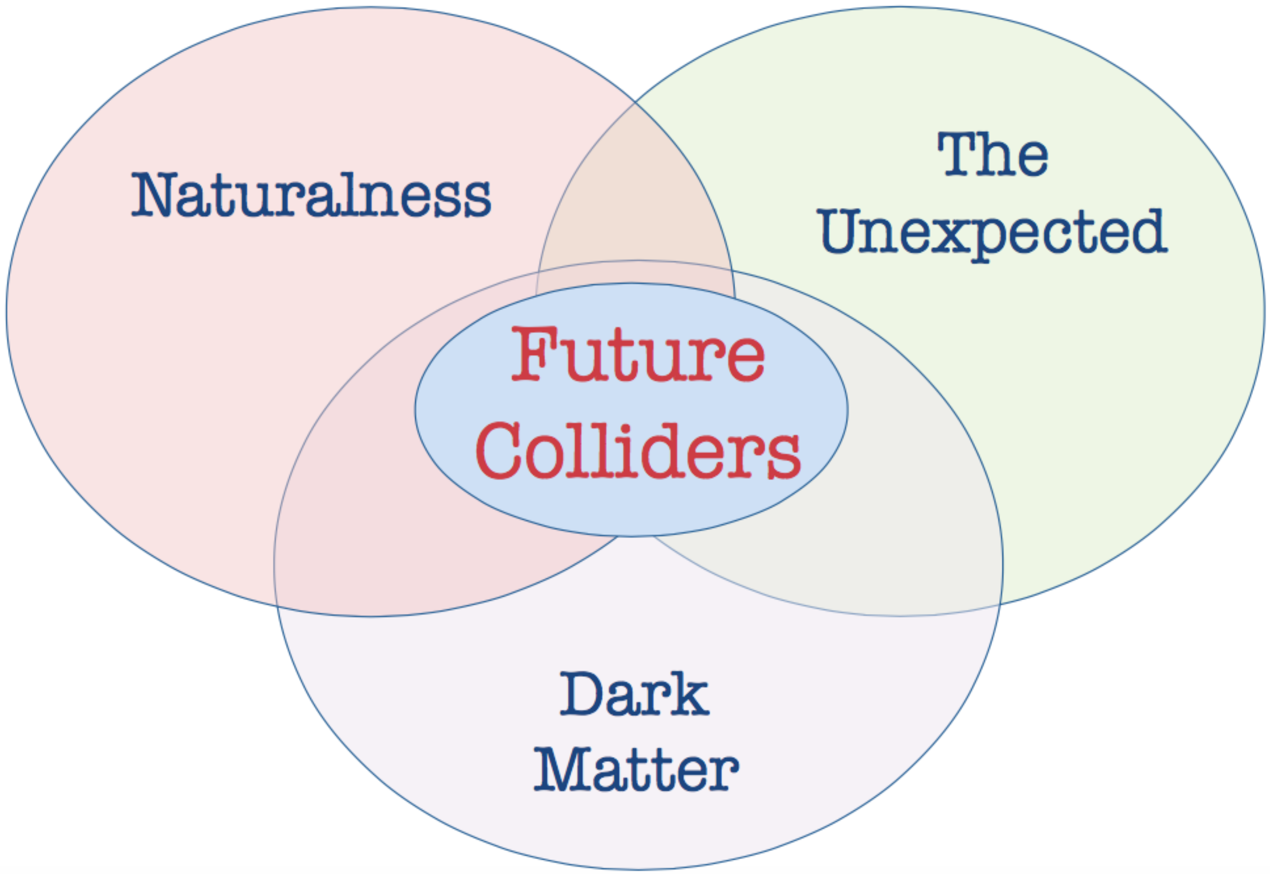

DiHiggs 2020 – Opportunities and Challenges
T. D. Lee Institute, Shanghai Jiao Tong University
November 20, 2020

Old and New Questions

- How to think of the vacuum as an "electroweak condensed state" ?
- How are the mysteries associated with a single, fundamental scalar field solved?
- What is the origin and nature of Dark Matter?
- What is the origin of the Baryon Asymmetry in the Universe?
- Why is Dark Energy so small but non-zero?
-
-

Fundamental *vs* Parametric Physics

- Fundamental principles lead to
  - Chiral fermions from irreducible representations of Lorentz group
    - fermions as spin ½ representations of Lorentz group
    - Fermi-Dirac statistics → Pauli Exclusion Principle
    - why matter occupies volume
  - Massless force mediators (gauge bosons) from gauge invariance
  - Massive gauge bosons and fermions from spontaneous breaking of gauge symmetry

- In comparison, the breaking of gauge symmetry by the Higgs VeV is parametrically induced
  - No dynamic or underlying principle behind it in the Standard Model

Why is Higgs Puzzling

Gauge sector $$L = i\bar{\psi}\gamma^{\mu}D_{\mu}\psi - \frac{1}{2}F_{\mu\nu}F^{\mu\nu}$$

particle	spin
quark: u, d,...	1/2
lepton: e...	1/2
photon	1
W,Z	1
gluon	1
Higgs	0

h: a new kind of
elementary particle

Higgs sector
$$L = \left(h_{ij}\bar{\psi}_i\psi_j H + \text{h.c.}\right) - \lambda|H|^4 + \mu^2|H|^2 - \Lambda_{CC}^4$$

Why is Higgs Puzzling

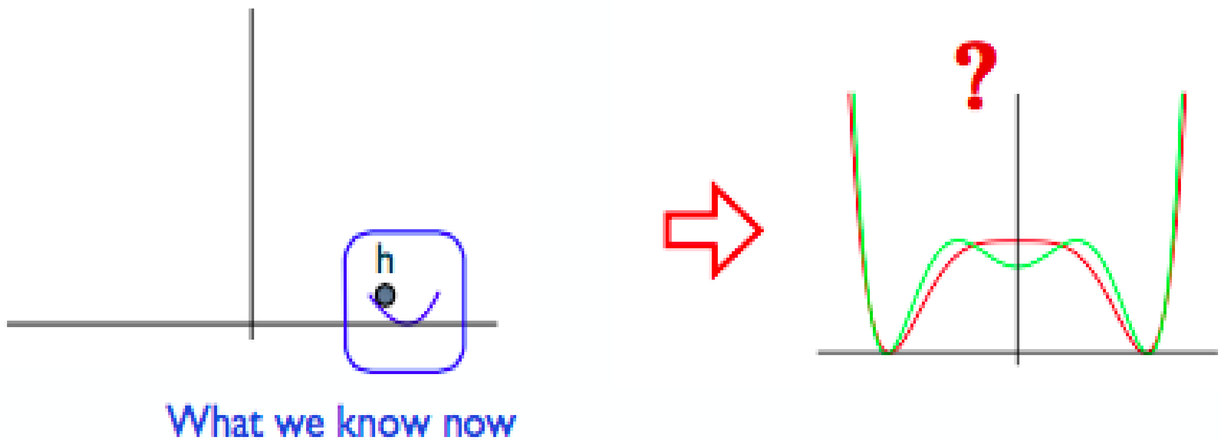

$$V(h) = \frac{1}{2}\mu^2 h^2 + \frac{\lambda}{4} h^4 \quad \text{or} \quad V(h) = \frac{1}{2}\mu^2 h^2 + \frac{\lambda}{4} h^4 + \frac{1}{\Lambda^2} h^6$$

Ad-hoc potential, similar to and motivated by Landau-Ginzburg theory of superconductivity

Higgs potential in SM can be extrapolated to Planck scale without additional parameters; but no a-priori reason for a parameterization to respect this condition

Higgs boson puzzles

- First fundamental (?) scalar field to be discovered
- Spontaneous symmetry breaking by development of a VeV
  - But VeV is induced parametrically by ad-hoc Higgs potential, no dynamics
- Parameters of Higgs potential are not stable under radiative corrections
  - First time that the radiative correction to a particle mass is additive and quadratically divergent
  - Gauge boson masses are protected by gauge invariance
  - Fermion masses are protected by chiral symmetry of massless fermions
- Single scalar Higgs field is a strange beast, compared to fermions and gauge bosons
- Additional symmetries and/or dynamics strongly motivated by Higgs discovery

Circular *pp* Collider

Circular *pp* Collider Physics Goals

- Testable reasons why the Standard Model must be incomplete
  - Dark Matter could be
    - Weakly-interacting particles
    - Particles interacting through Higgs portal
    - Interacting with SM particles through gravity
  - Electroweak Baryogenesis
    - Can the electroweak phase transition (formation of Higgs VeV) provide the out-of-equilibrium condition needed for matter-antimatter asymmetry observed?
  - Can the parameter space of new physics be a bounded parameter space?
    - Can it be fully covered with a 100-TeV scale *pp* collider?
- Naturalness – the need to explain the lightness of the Higgs mass – testing Naturalness at 10^{-4}

Higgs Self-Coupling

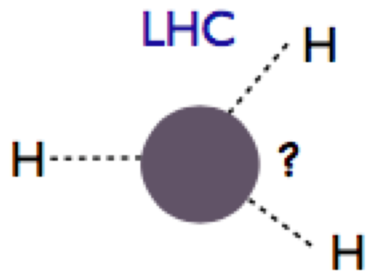

Unique type of coupling for spin-0 scalars
Not seen before in nature!

Measuring it well is crucial to answer this question.

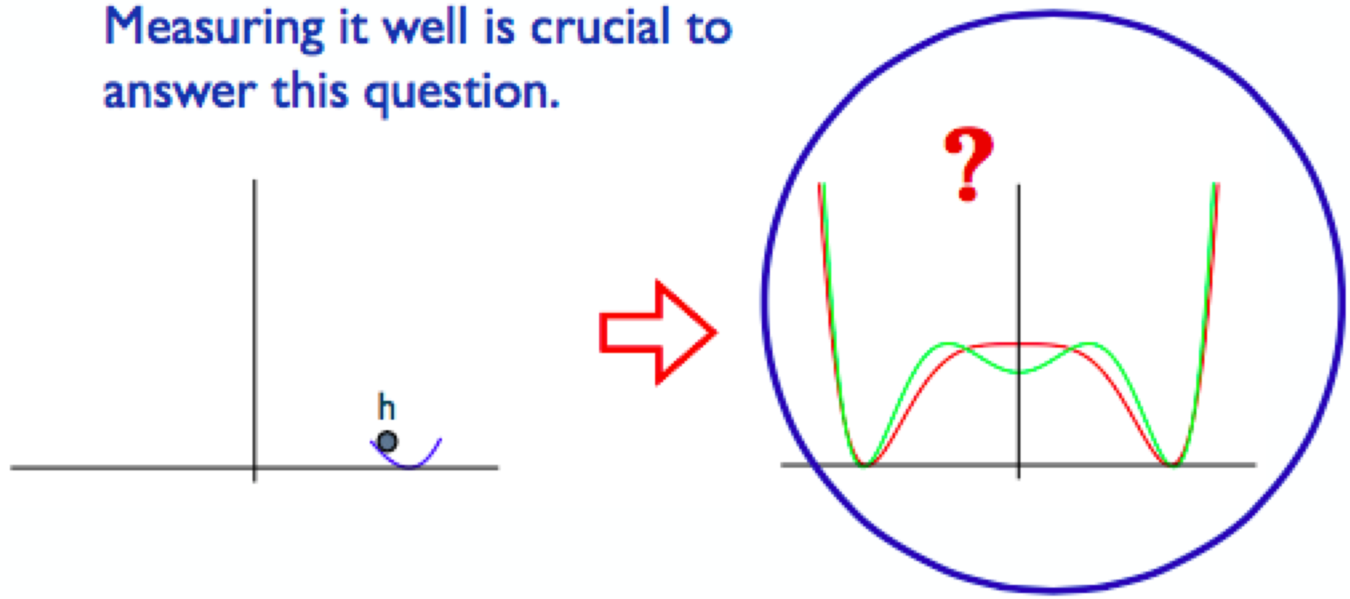

Expect $O(1)$ deviations from SM in self-coupling coefficient

Rate comparisons at 8, 14, 100 TeV

	N_{100}	N_{100}/N_8	N_{100}/N_{14}
gg→H	16 G	4.2×10^4	110
VBF	1.6 G	5.1×10^4	120
WH	320 M	2.3×10^4	66
ZH	220 M	2.8×10^4	84
ttH	760 M	29×10^4	420
gg→HH	28 M		280

$N_{100} = \sigma_{100\,\text{TeV}} \times 20\ \text{ab}^{-1}$

$N_8 = \sigma_{8\,\text{TeV}} \times 20\ \text{fb}^{-1}$

$N_{14} = \sigma_{14\,\text{TeV}} \times 3\ \text{ab}^{-1}$

Statistical precision:

- O(100 - 500) better w.r.t Run 1
- O(10 - 20) better w.r.t HL-LHC

Measuring the Higgs Self-Coupling

- gg→HH (most promising?) , qq→HHqq (via VBF)
- Reference benchmark process: HH→bb γγ
- Goal: 5% (or better) precision for SM selfcoupling

$HH \rightarrow b\bar{b}\gamma\gamma$	Barr,Dolan,Englert,Lima, Spannowsky JHEP 1502 (2015) 016	Contino, Azatov, Panico, Son arXiv:1502.00539	He, Ren Yao arXiv:1506.03302
FCC$_{@100\mathrm{TeV}}$ 3/ab	30~40%	30%	15%
FCC$_{@100\mathrm{TeV}}$ 30/ab	10%	10%	5%
$S/\sqrt{B}$	8.4	15.2	16.5
Details	✓ λ_{HHH} modification only ✓ $c \rightarrow b$ & $j \rightarrow \gamma$ included ✓ Background systematics ○ $b\bar{b}\gamma\gamma$ not matched ✓ $m_{\gamma\gamma} = 125 \pm 1$ GeV	✓ Full EFT approach ○ No $c \rightarrow b$ & $j \rightarrow \gamma$ ✓ Marginalized ✓ $b\bar{b}\gamma\gamma$ matched ✓ $m_{\gamma\gamma} = 125 \pm 5$ GeV ✓ Jet /W_{had} veto	✓ λ_{HHH} modification only ✓ $c \rightarrow b$ & $j \rightarrow \gamma$ included ○ No marginalization ✓ $b\bar{b}\gamma\gamma$ matched ✓ $m_{\gamma\gamma} = 125 \pm 3$ GeV

Work in progress to compare studies, harmonize performance assumptions, optimize, etc ⇒ ideal benchmarking framework

Origin of Matter-Antimatter Asymmetry

Origin of Baryon Asymmetry

POSSIBLE EXPLANATIONS...

$$\frac{n_B - n_{\bar{B}}}{n_\gamma} \sim 10^{-9} \text{ (from BBN)}$$

⇨ **Baryogenesis at EW Scale** → **TESTABLE!**

⇨ ...

SAKHAROV CONDITIONS (for dynamical generation of baryon asymmetry)

B Violation ✓ Sphalerons

V. A. Kuzmin, V. A. Rubakov, M. Shaposhnikov, Phys. Lett. B**155** (1985) 36

C/CP Violation ✗ not enough

Departure from Thermal Equilibrium ✗ not enough

Baryon Asymmetry and Electroweak Phase Transition

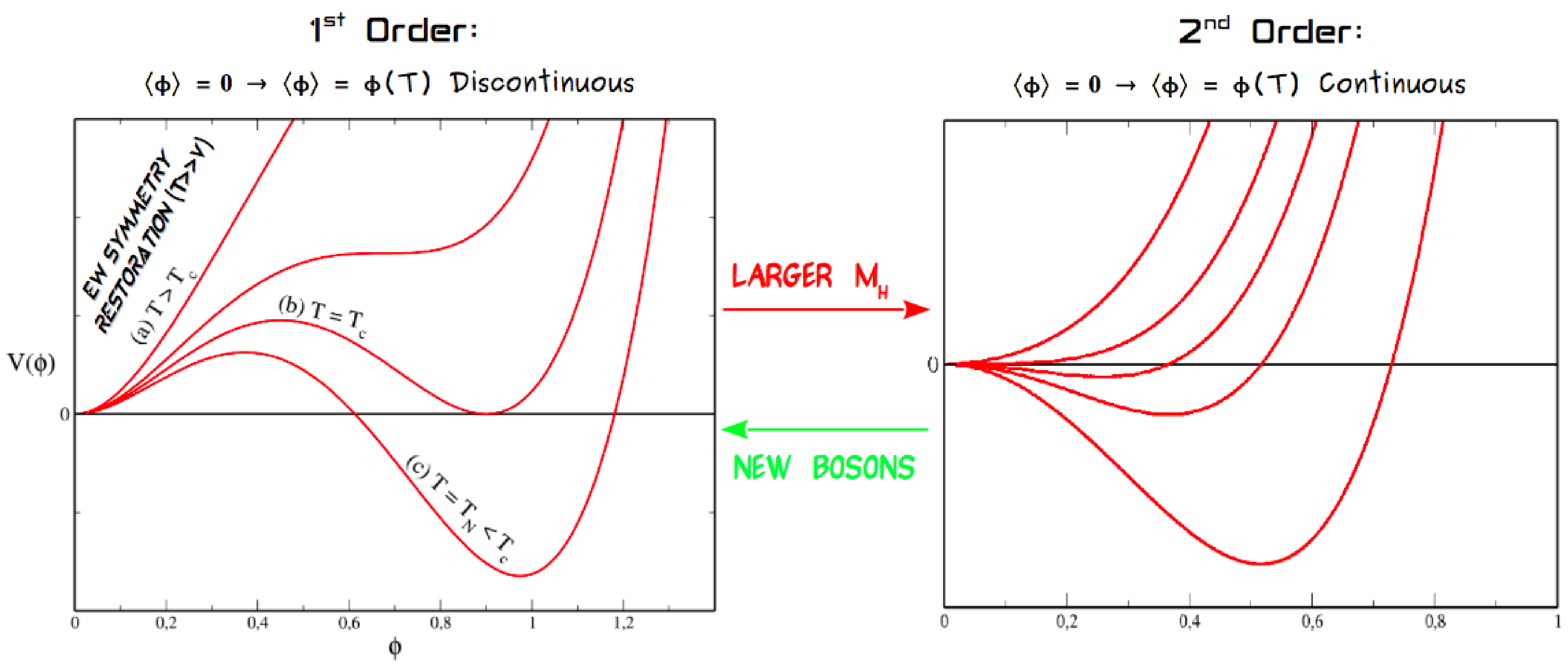

In the SM **(m_h = 125 GeV)** EW Phase Transition Smooth CrossOver

K. Kajantie, M. Laine, K. Rummukainen, M. Shaposhnikov, Phys. Rev. Lett. ***77*** *(1996) 2887*

Baryon Asymmetry and Electroweak Phase Transition

1^{st} Order:

$\langle\phi\rangle = 0 \rightarrow \langle\phi\rangle = \phi(T)$ Discontinuous

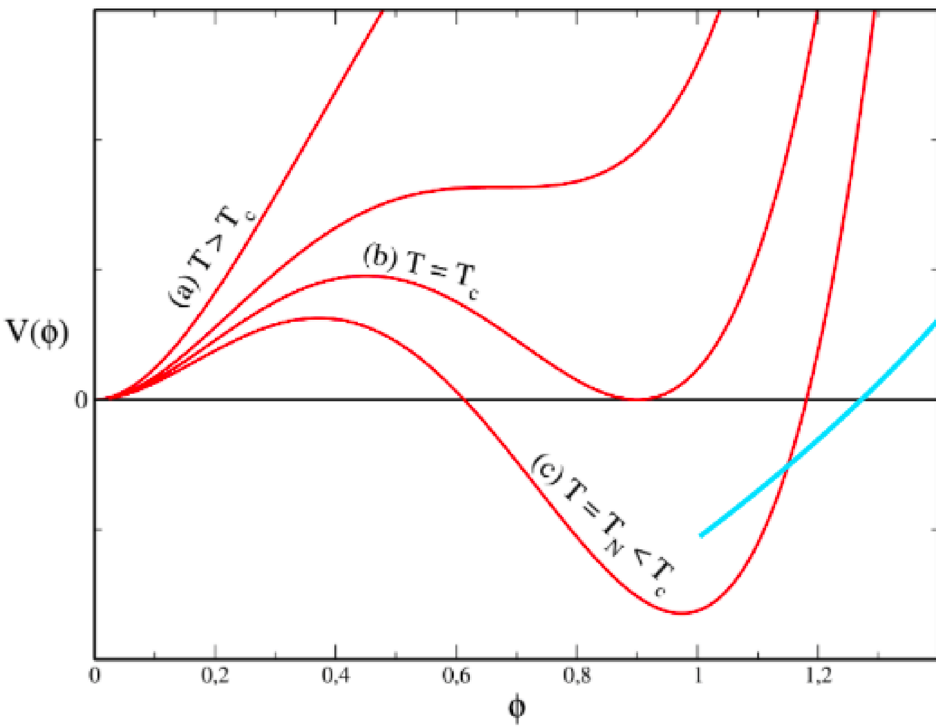

Nucleation of True Vacuum Bubbles (in False Vacuum Sea)

J. S. Langer, Ann. Phys. ***54*** *(1969) 258*

S. R. Coleman, Phys. Rev. D ***15*** *(1977) 2929*

A. D. Linde, Nucl. Phys. B ***216*** *(1983) 421*

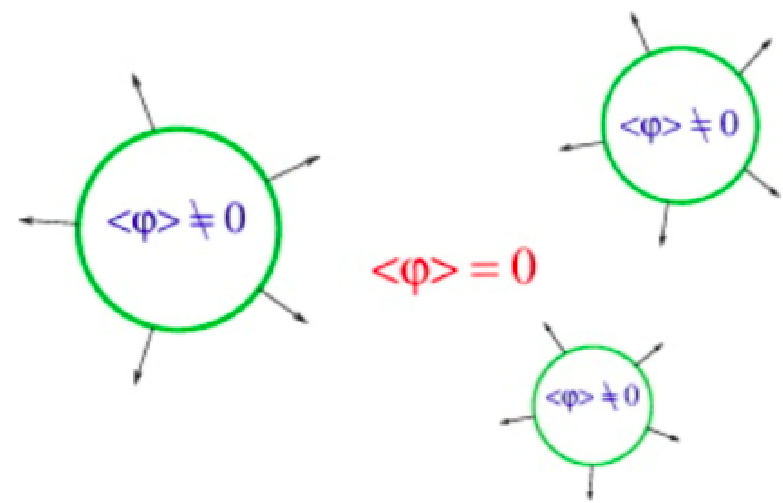

SUDDEN CHANGE IN HIGGS VEV

Inducing First-Order Electroweak Phase Transition

$$V(H,S) = -\mu^2\left(H^\dagger H\right) + \lambda\left(H^\dagger H\right)^2 + \frac{a_1}{2}\left(H^\dagger H\right)S$$
$$+\frac{a_2}{2}\left(H^\dagger H\right)S^2 + \frac{b_2}{2}S^2 + \frac{b_3}{3}S^3 + \frac{b_4}{4}S^4$$

$$m_h^2 \equiv \frac{d^2V}{dh^2} = 2\lambda v_0^2$$
$$m_s^2 \equiv \frac{d^2V}{ds^2} = b_3 x_0 + 2b_4 x_0^2 - \frac{a_1 v_0^2}{4x_0}$$
$$m_{hs}^2 \equiv \frac{d^2V}{dhds} = (a_1 + 2a_2 x_0)\,\frac{v_0}{2}. \qquad (5)$$

with m_{hs}^2 being responsible for the singlet-doublet mixing. The corresponding mass eigenstates are given by

$$h_1 = h\cos\theta + s\sin\theta$$
$$h_2 = -h\sin\theta + s\cos\theta \qquad (6)$$

(AVK, M.J.Ramsey-Musolf, J.M. No, P.Winslow, *Phys. Rev.D* 94 (2016) 3, 035022)

Inducing First-Order Electroweak Phase Transition

$$V(H,S) = -\mu^2\left(H^\dagger H\right) + \lambda\left(H^\dagger H\right)^2 + \frac{a_1}{2}\left(H^\dagger H\right)S$$
$$+\frac{a_2}{2}\left(H^\dagger H\right)S^2 + \frac{b_2}{2}S^2 + \frac{b_3}{3}S^3 + \frac{b_4}{4}S^4$$

$$\lambda_{211} = \frac{1}{4}\left[(a_1 + 2a_2x_0)\cos^3\theta + 4v_0(a_2 - 3\lambda)\cos^2\theta\sin\theta \right.$$
$$\left. +(a_1 + 2a_2x_0 - 2b_3 - 6b_4x_0)\cos\theta\sin^2\theta - 2a_2v_0\sin^3\theta\right] \tag{12}$$

and, along with the $\sin^2\theta$ rescaling, modifies the rate associated with the heavy Higgs production and decay. The partial width $\Gamma_{h_2\to h_1h_1}$ is given by

$$\Gamma_{h_2\to h_1h_1} = \frac{\lambda_{211}^2\sqrt{1-4m_1^2/m_2^2}}{8\pi m_2}. \tag{13}$$

(AVK, M.J.Ramsey-Musolf, J.M. No, P.Winslow, *Phys. Rev.D* 94 (2016) 3, 035022)

Inducing First-Order Electroweak Phase Transition

$$V(H,S) = -\mu^2\left(H^\dagger H\right) + \lambda\left(H^\dagger H\right)^2 + \frac{a_1}{2}\left(H^\dagger H\right)S$$
$$+\frac{a_2}{2}\left(H^\dagger H\right)S^2 + \frac{b_2}{2}S^2 + \frac{b_3}{3}S^3 + \frac{b_4}{4}S^4$$

Defining $\Gamma^{\rm SM}(m_2)$ as the SM Higgs width evaluated at m_2, which we take from [34], the total width for the h_2 boson is given by

$$\Gamma_{h_2} = \sin^2\theta\,\Gamma^{\rm SM}(m_2) + \Gamma_{h_2\to h_1 h_1}. \qquad (14)$$

The resulting signal rate (normalized to the SM value) for $pp \to h_2 \to XX$ (with XX representing all SM final states except $h_1 h_1$) is

$$\mu_{h_2\to XX} = \sin^2\theta\left(\frac{\sin^2\theta\,\Gamma^{\rm SM}(m_2)}{\Gamma_{h_2}}\right). \qquad (15)$$

(AVK, M.J.Ramsey-Musolf, J.M. No, P.Winslow, *Phys. Rev.D* 94 (2016) 3, 035022)

First Order Phase Transition

$$V(H,S) = -\mu^2\left(H^\dagger H\right) + \lambda\left(H^\dagger H\right)^2 + \frac{a_1}{2}\left(H^\dagger H\right)S + \frac{a_2}{2}\left(H^\dagger H\right)S^2 + \frac{b_2}{2}S^2 + \frac{b_3}{3}S^3 + \frac{b_4}{4}S^4$$

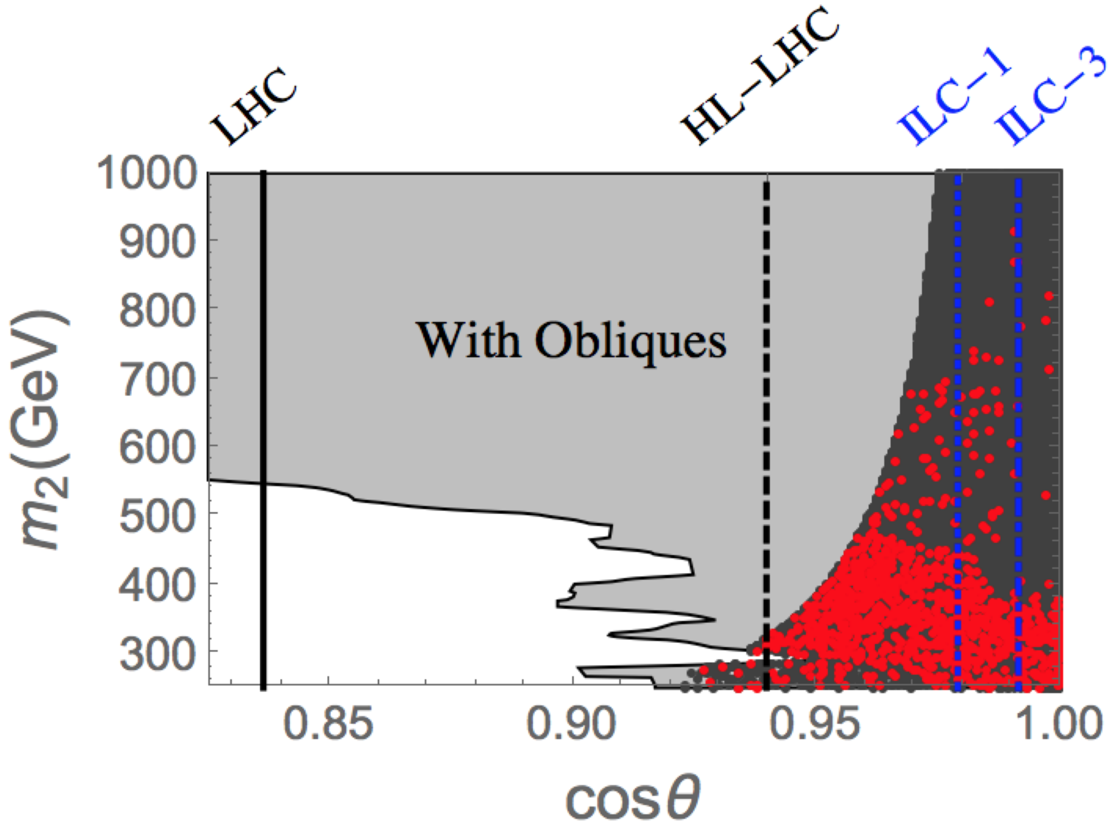

(from P. Winslow)

S. Profumo, M. J. Ramsey-Musolf, C. L. Wainwright and P. Winslow, arXiv:1407.5342

Can TeV-scale new physics associated with 1st order phase transition be completely covered by a *pp* collider?

Inducing First-Order Electroweak Phase Transition

$$V(H,S) = -\mu^2\left(H^\dagger H\right) + \lambda\left(H^\dagger H\right)^2 + \frac{a_1}{2}\left(H^\dagger H\right)S + \frac{a_2}{2}\left(H^\dagger H\right)S^2 + \frac{b_2}{2}S^2 + \frac{b_3}{3}S^3 + \frac{b_4}{4}S^4$$

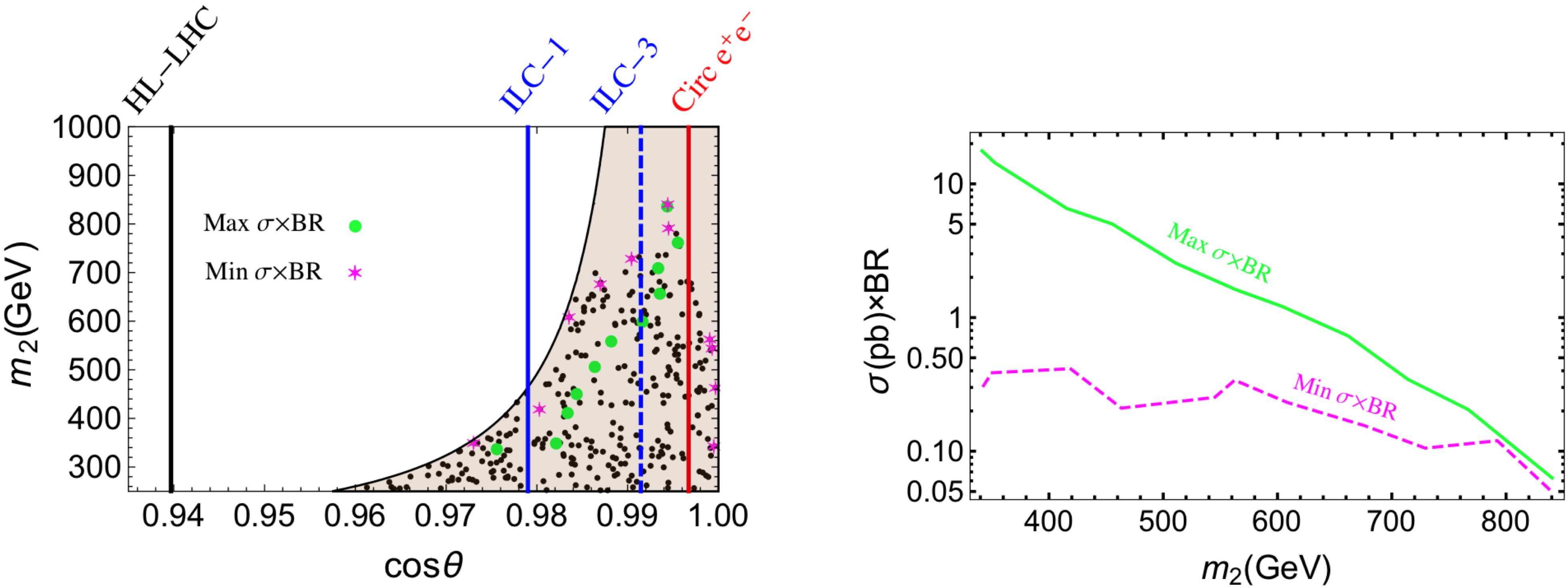

FIG. 1: Left pane: Distribution of SFOEWPT points in m_2 *vs* $\cos\theta$ space. Maximum (minimum) benchmark points are shown in green (magenta). Right pane: Maximum (minimum) cross section times branching ratio as a function of m_2 at a 100 TeV pp collider, taken from Table I (Table II), is displayed as a solid green (dashed magenta) line.

(AVK, M.J.Ramsey-Musolf, J.M. No, P.Winslow, *Phys. Rev.D* 94 (2016) 3, 035022)

DiHiggs Branching Ratios

Decay channel	Branching ratio	Uncertainty
$b\bar{b}b\bar{b}$	$3.33 \cdot 10^{-1}$	$\pm 2.20 \cdot 10^{-2}$
$\tau\tau b\bar{b}$	$7.29 \cdot 10^{-2}$	$\pm 4.80 \cdot 10^{-3}$
$W^+(\to l\nu)W^-(\to l\nu)b\bar{b}$	$1.09 \cdot 10^{-2}$	$\pm 5.93 \cdot 10^{-4}$
$\tau\tau\tau\tau$	$3.99 \cdot 10^{-3}$	$\pm 4.55 \cdot 10^{-4}$
$\gamma\gamma b\bar{b}$	$2.63 \cdot 10^{-3}$	$\pm 1.58 \cdot 10^{-4}$
$W^+(\to l\nu)W^-(\to l\nu)\tau\tau$	$1.20 \cdot 10^{-3}$	$\pm 8.56 \cdot 10^{-5}$
$\gamma\gamma\tau\tau$	$2.88 \cdot 10^{-4}$	$\pm 2.19 \cdot 10^{-5}$
$b\bar{b}\mu^+\mu^-$	$2.53 \cdot 10^{-4}$	$\pm 1.73 \cdot 10^{-5}$
$Z(\to l^+l^-)Z(\to l^+l^-)b\bar{b}$	$1.41 \cdot 10^{-4}$	$\pm 7.64 \cdot 10^{-6}$
$b\bar{b}Z(\to l^+l^-)\gamma$	$1.21 \cdot 10^{-4}$	$\pm 1.16 \cdot 10^{-5}$
$W^+(\to l\nu)W^-(\to l\nu)W^+(\to l\nu)W^-(\to l\nu)$	$8.99 \cdot 10^{-5}$	$\pm 7.73 \cdot 10^{-6}$
$\gamma\gamma W^+(\to l\nu)W^-(\to l\nu)$	$4.32 \cdot 10^{-5}$	$\pm 2.85 \cdot 10^{-6}$
$\tau\tau\mu^+\mu^-$	$2.77 \cdot 10^{-5}$	$\pm 2.29 \cdot 10^{-6}$
$Z(\to l^+l^-)Z(\to l^+l^-)\tau\tau$	$1.54 \cdot 10^{-5}$	$\pm 1.10 \cdot 10^{-6}$
$\tau\tau Z(\to l^+l^-)\gamma$	$1.32 \cdot 10^{-5}$	$\pm 1.41 \cdot 10^{-6}$
$\gamma\gamma\gamma\gamma$	$5.20 \cdot 10^{-6}$	$\pm 5.20 \cdot 10^{-7}$
$W^+(\to l\nu)W^-(\to l\nu)\mu^+\mu^-$	$4.15 \cdot 10^{-6}$	$\pm 3.07 \cdot 10^{-7}$
$Z(\to l^+l^-)Z(\to l^+l^-)W^+(\to l\nu)W^-(\to l\nu)$	$2.31 \cdot 10^{-6}$	$\pm 1.41 \cdot 10^{-7}$
$W^+(\to l\nu)W^-(\to l\nu)Z(\to l^+l^-)\gamma$	$1.99 \cdot 10^{-6}$	$\pm 1.98 \cdot 10^{-7}$
$\gamma\gamma\mu^+\mu^-$	$9.99 \cdot 10^{-7}$	$\pm 7.80 \cdot 10^{-8}$
$\gamma\gamma Z(\to l^+l^-)Z(\to l^+l^-)$	$5.57 \cdot 10^{-7}$	$\pm 3.67 \cdot 10^{-8}$
$\gamma\gamma Z(\to l^+l^-)\gamma$	$4.78 \cdot 10^{-7}$	$\pm 4.92 \cdot 10^{-8}$
$Z(\to l^+l^-)Z(\to l^+l^-)\mu^+\mu^-$	$5.35 \cdot 10^{-8}$	$\pm 3.95 \cdot 10^{-9}$
$Z(\to l^+l^-)\gamma\mu^+\mu^-$	$4.59 \cdot 10^{-8}$	$\pm 4.96 \cdot 10^{-9}$
$Z(\to l^+l^-)Z(\to l^+l^-)Z(\to l^+l^-)\gamma$	$2.56 \cdot 10^{-8}$	$\pm 2.55 \cdot 10^{-9}$
$Z(\to l^+l^-)Z(\to l^+l^-)Z(\to l^+l^-)Z(\to l^+l^-)$	$1.49 \cdot 10^{-8}$	$\pm 1.28 \cdot 10^{-9}$
$Z(\to l^+l^-)\gamma Z(\to l^+l^-)\gamma$	$1.10 \cdot 10^{-8}$	$\pm 1.97 \cdot 10^{-9}$

HH → bbγγ

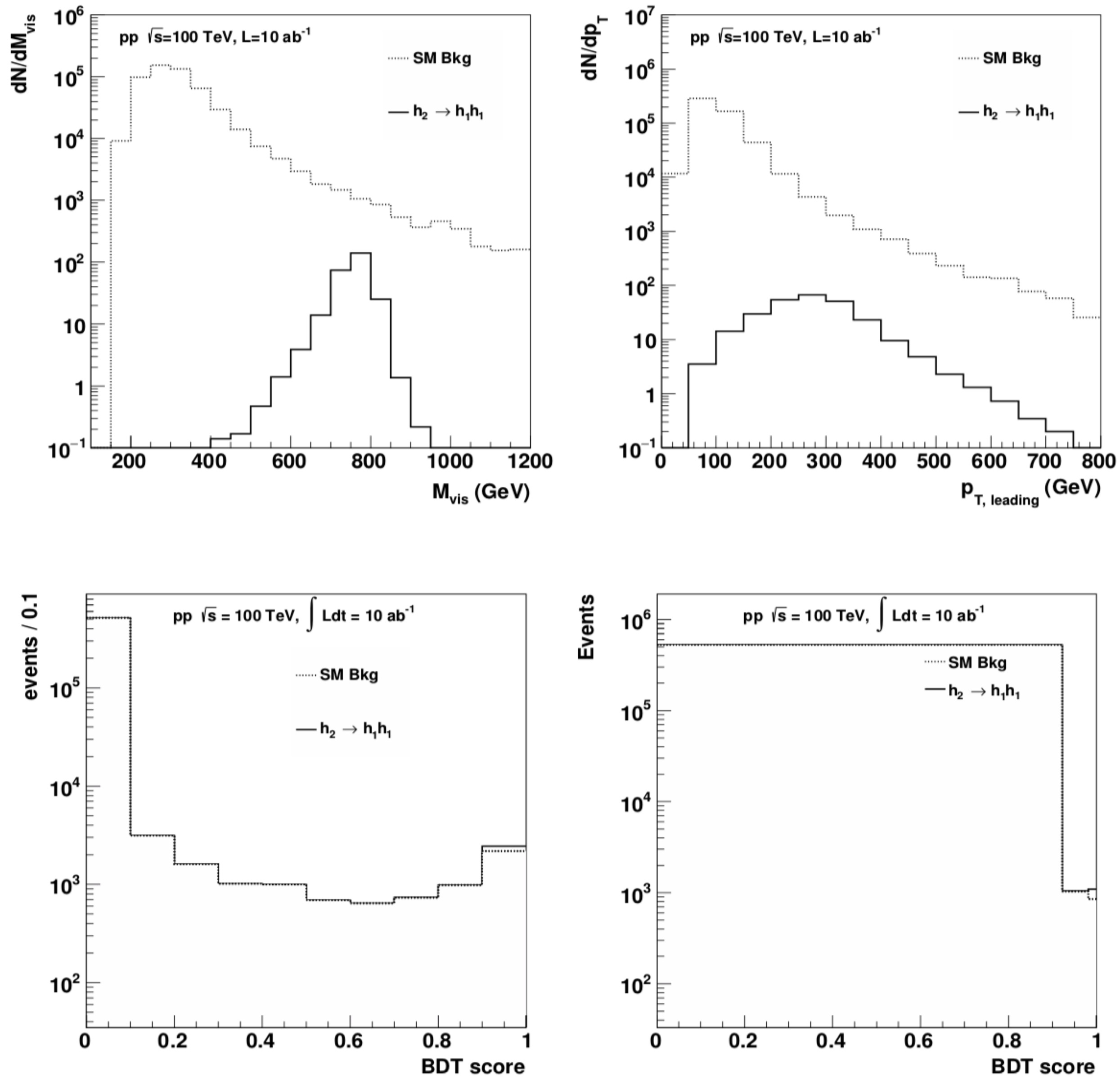

FIG. 2: Signal and background distributions for the $b\bar{b}\gamma\gamma$ final state. The signal distributions correspond to $\mathrm{BM10}^{\mathrm{max}}$. The kinematic quantities shown are (top left) the invariant mass of the $b\bar{b}\gamma\gamma$ system, and (top right) the p_T of the leading particle from among the photons and the b-quarks. Also shown are the distributions of the BDT output with uniform binning (bottom left) and optimized binning (bottom right).

HH → bbγγ

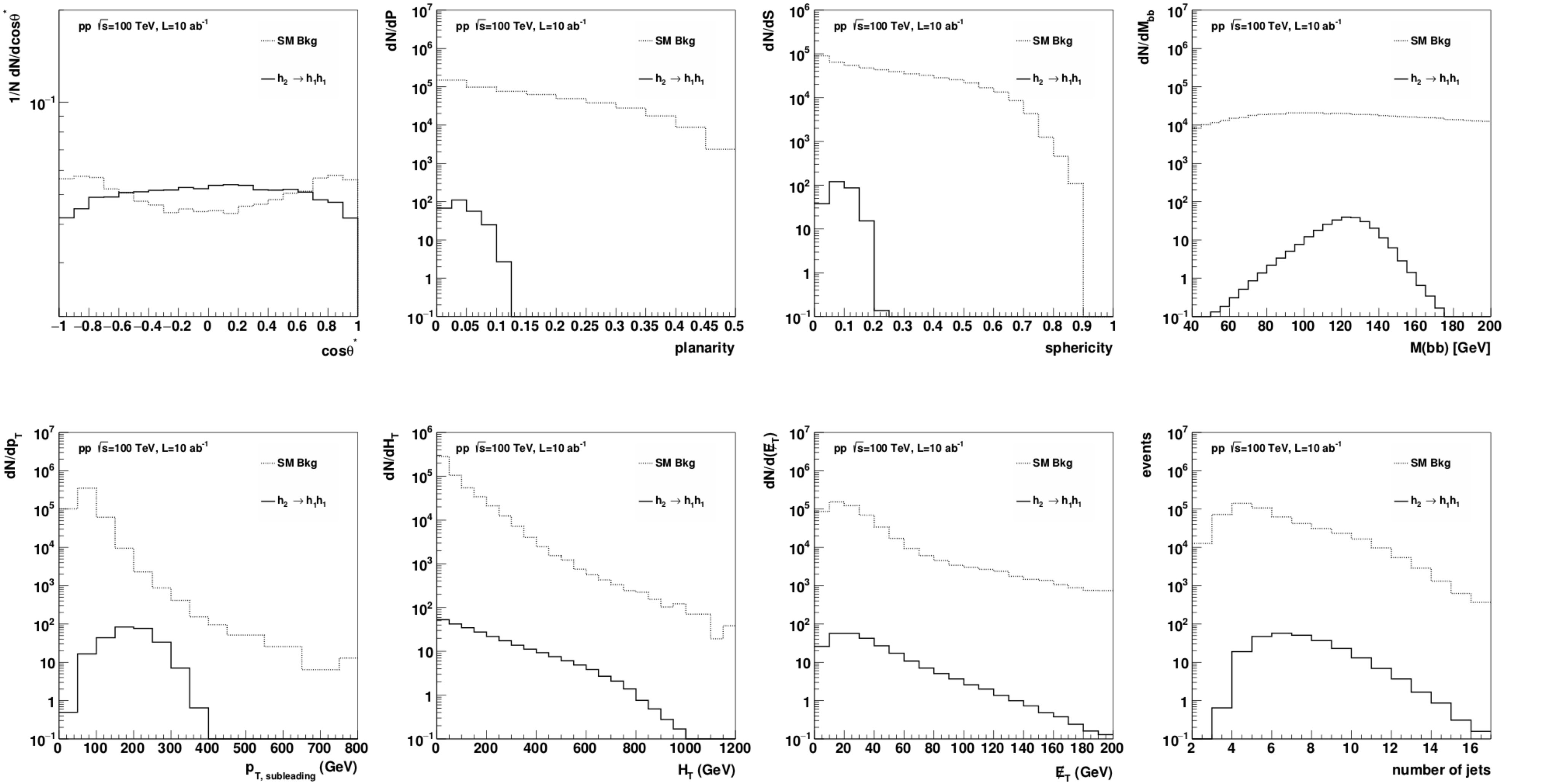

FIG. 7: Additional kinematics distributions for $b\bar{b}\gamma\gamma$ final state, used as inputs to the BDT. The signal distributions correspond to BM10$^{\rm max}$.

(AVK, M.J.Ramsey-Musolf, J.M. No, P.Winslow, *Phys. Rev.D* 94 (2016) 3, 035022)

HH → bbγγ

$$V(H,S) = -\mu^2\left(H^\dagger H\right) + \lambda\left(H^\dagger H\right)^2 + \frac{a_1}{2}\left(H^\dagger H\right)S$$
$$+\frac{a_2}{2}\left(H^\dagger H\right)S^2 + \frac{b_2}{2}S^2 + \frac{b_3}{3}S^3 + \frac{b_4}{4}S^4$$

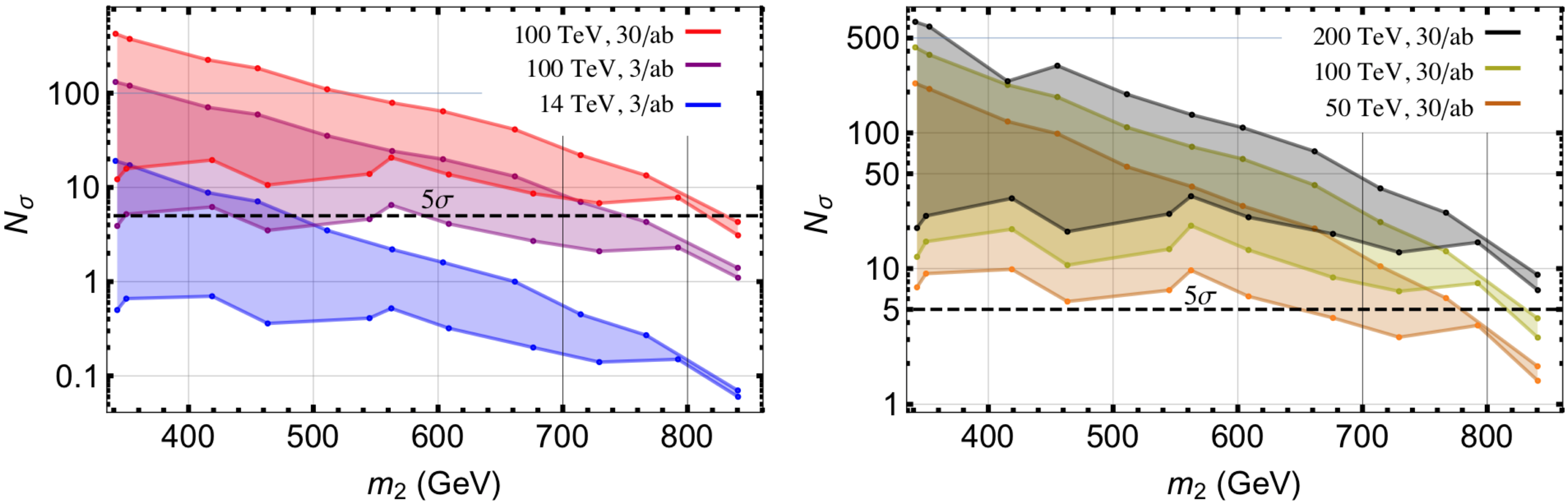

FIG. 3: The N_σ gaussian significance for rejecting the background-only hypothesis, obtained using the $b\bar{b}\gamma\gamma$ final state, for each benchmark point. Different collider scenarios of energy and integrated luminosity are compared. The vertical range corresponds to the maximum and minimum signal cross sections in the h_2 mass window.

(AVK, M.J.Ramsey-Musolf, J.M. No, P.Winslow, *Phys. Rev.D* 94 (2016) 3, 035022)

$H \to 4\tau$

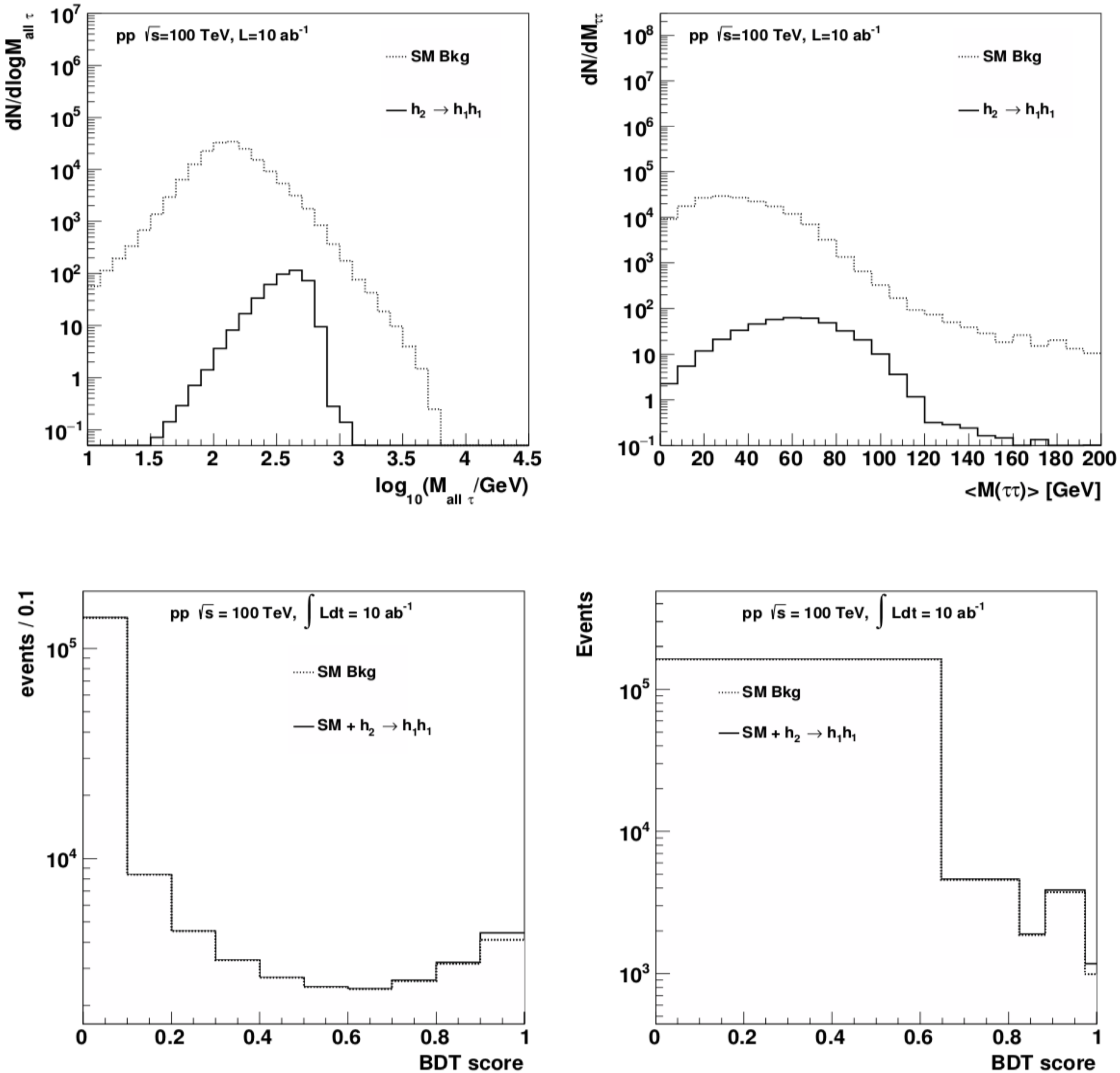

FIG. 4: Signal and background distributions for the 4τ final state, where the signal corresponds to BM10$^{\text{max}}$. The kinematic quantities shown are (top left) the invariant mass of the 4τ system, and (top right) the average di-τ pair mass in the event. Also shown are the distributions of the BDT output with uniform binning (bottom left) and optimized binning (bottom right).

$H \to 4\,\tau$

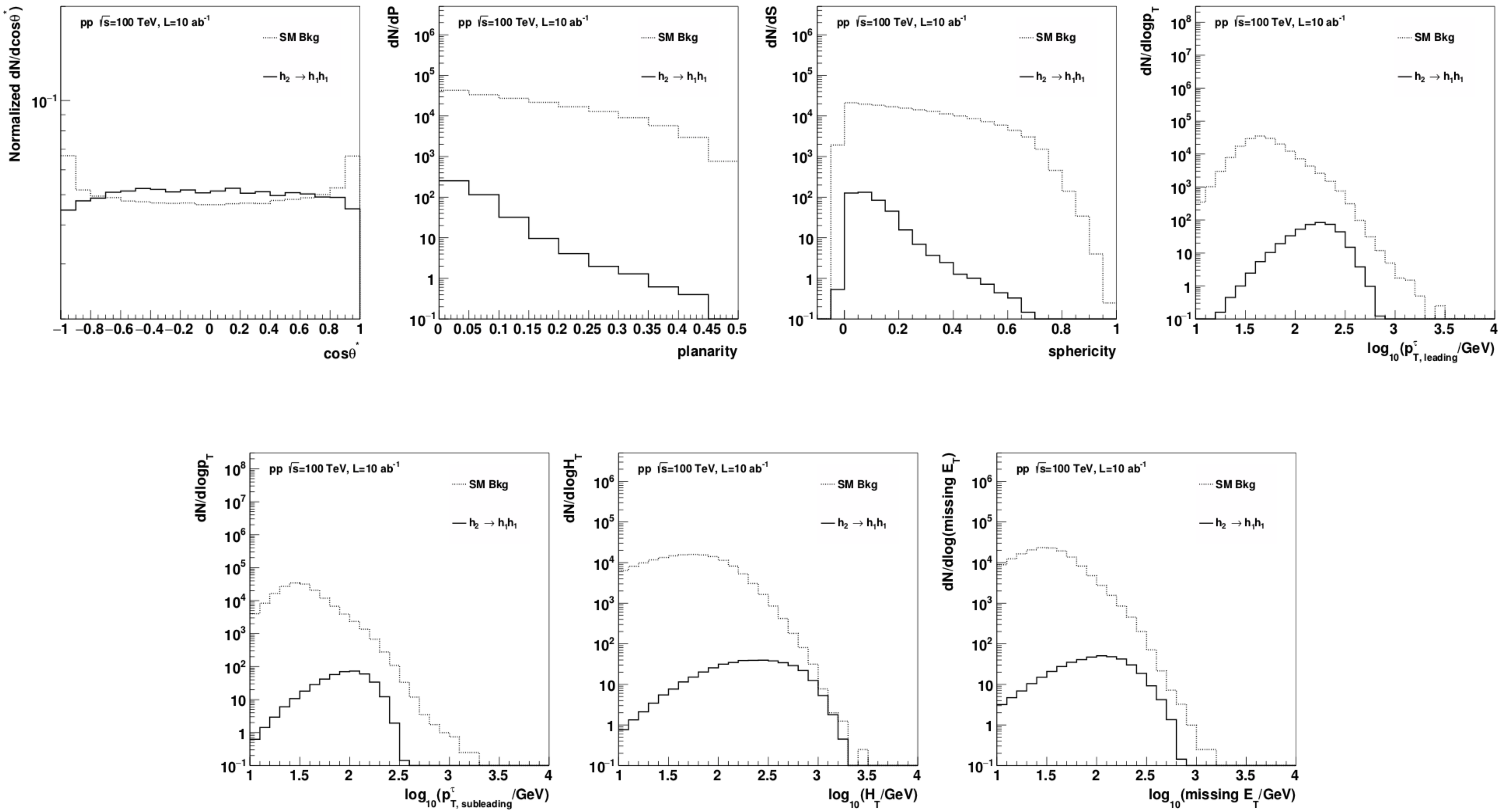

FIG. 8: Additional kinematics distributions for 4τ final state, used as inputs to the BDT. The signal distributions correspond to $\mathrm{BM10}^{\mathrm{max}}$.

$H \to 4\tau$

$$V(H,S) = -\mu^2 \left(H^\dagger H\right) + \lambda \left(H^\dagger H\right)^2 + \frac{a_1}{2}\left(H^\dagger H\right) S + \frac{a_2}{2}\left(H^\dagger H\right) S^2 + \frac{b_2}{2} S^2 + \frac{b_3}{3} S^3 + \frac{b_4}{4} S^4$$

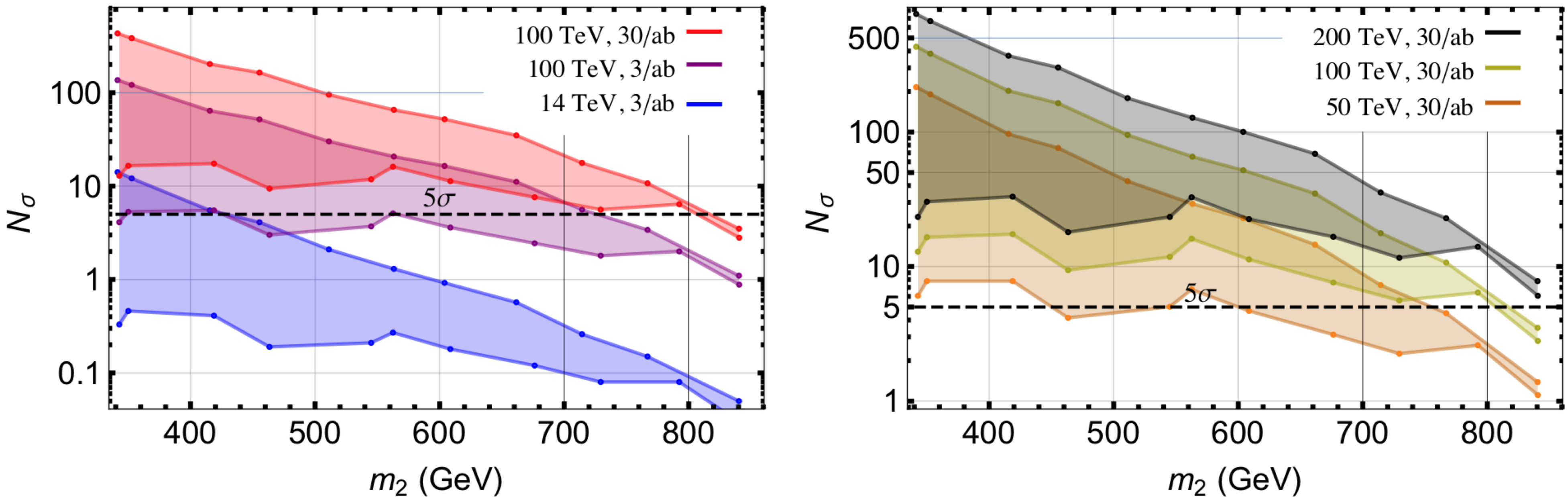

FIG. 5: The N_σ gaussian significance for rejecting the background-only hypothesis, obtained using the 4τ final state, for each benchmark point. Different collider scenarios of energy and integrated luminosities are compared. The vertical range corresponds to the maximum and minimum signal cross sections in the h_2 mass window.

(AVK, M.J.Ramsey-Musolf, J.M. No, P.Winslow, *Phys. Rev.D* 94 (2016) 3, 035022)

Inducing First-Order Electroweak Phase Transition

$$V(H,S) = -\mu^2\left(H^\dagger H\right) + \lambda\left(H^\dagger H\right)^2 + \frac{a_1}{2}\left(H^\dagger H\right)S$$
$$+\frac{a_2}{2}\left(H^\dagger H\right)S^2 + \frac{b_2}{2}S^2 + \frac{b_3}{3}S^3 + \frac{b_4}{4}S^4$$

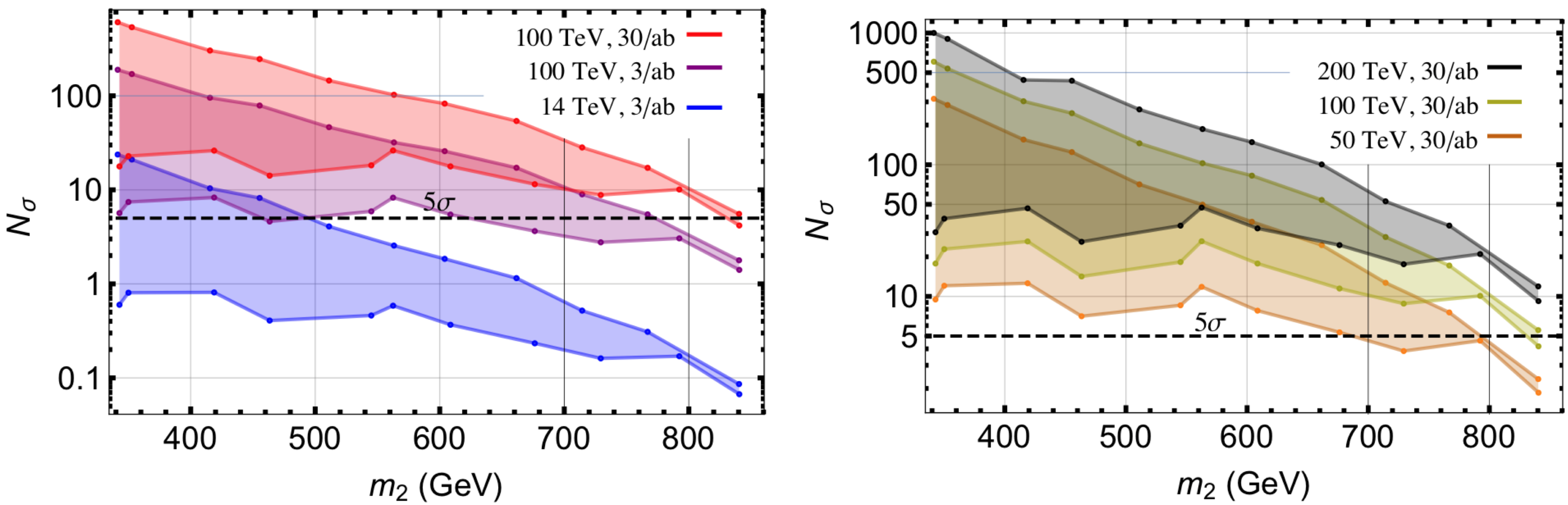

FIG. 6: The N_σ gaussian significance for rejecting the background-only hypothesis, obtained using the combination of the $b\bar{b}\gamma\gamma$ and 4τ final states, for each benchmark point. Different collider scenarios of energy and integrated luminosities are compared. The vertical range corresponds to the maximum and minimum signal cross sections in the h_2 mass window.

(AVK, M.J.Ramsey-Musolf, J.M. No, P.Winslow, *Phys. Rev.D* 94 (2016) 3, 035022)

Inducing First-Order Electroweak Phase Transition

$$V(H,S) = -\mu^2\left(H^\dagger H\right) + \lambda\left(H^\dagger H\right)^2 + \frac{a_1}{2}\left(H^\dagger H\right)S + \frac{a_2}{2}\left(H^\dagger H\right)S^2 + \frac{b_2}{2}S^2 + \frac{b_3}{3}S^3 + \frac{b_4}{4}S^4$$

$S \to HH \to \gamma\gamma bb$ and 4τ

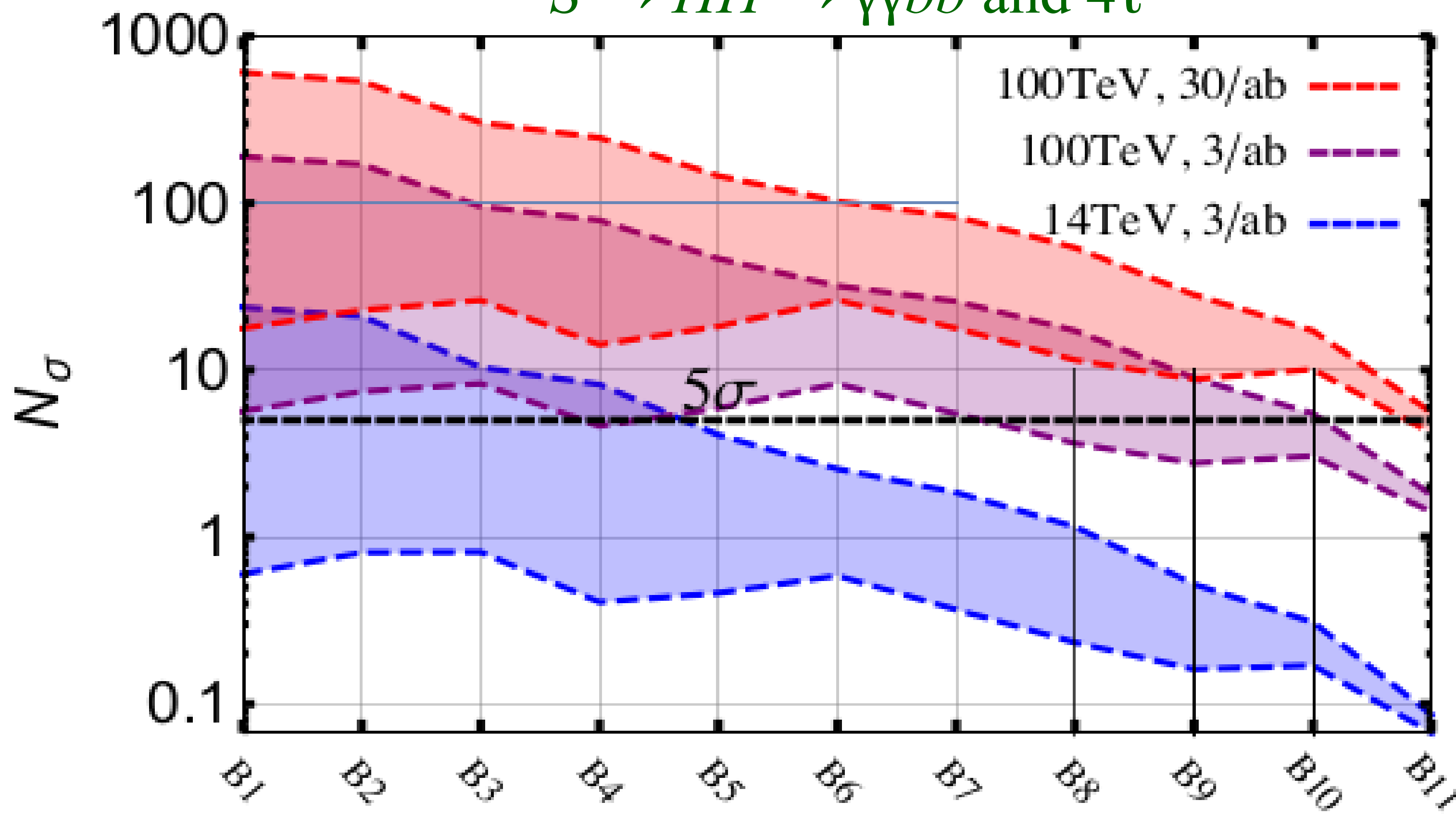

(P.Winslow, J.M. No, M.J.Ramsey-Musolf, AVK)

300 GeV ← benchmark m_s → 900 GeV

Discovery potential across entire parameter space

Why is the Higgs Boson So Light?

Why is the Higgs Boson So Light?

- Old idea: Higgs doublet (4 fields) is a Goldstone mode generated from the spontaneous breaking of a larger global symmetry
  - Higgs boson and W_L, Z_L are all Goldstone bosons from, eg. Spontaneously breaking global SO(5) → SO(4)
  - Examples: Holographic Higgs, Little Higgs models...
  - Electroweak vev "v" is small compared to SO(5) breaking scale "f"

- Vector boson scattering topology
  - Quarks emit longitudinal vector bosons which interact with new (presumably strong) dynamics
  - Quarks scatter by small angle in the forward direction

Longitudinal Vector Boson Scattering

Double Higgs Boson Production in the 4τChannel from Resonances in Longitudinal Vector Boson Scattering at a 100 TeV Collider

AVK, S. Chekanov, M. Low

Phys.Rev. D91 (2015) 114018

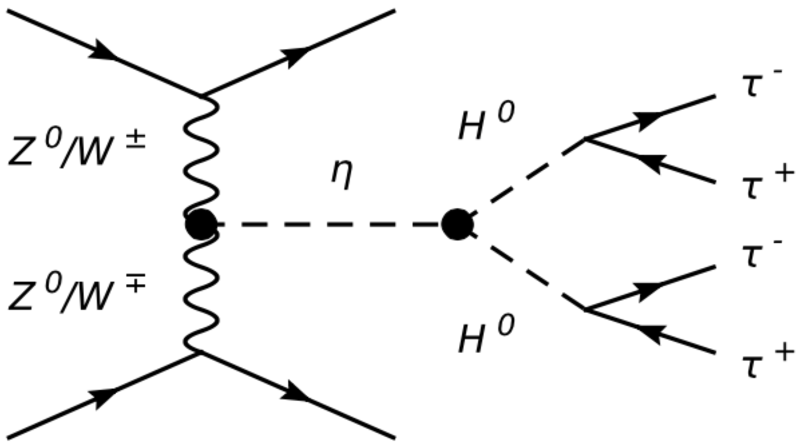

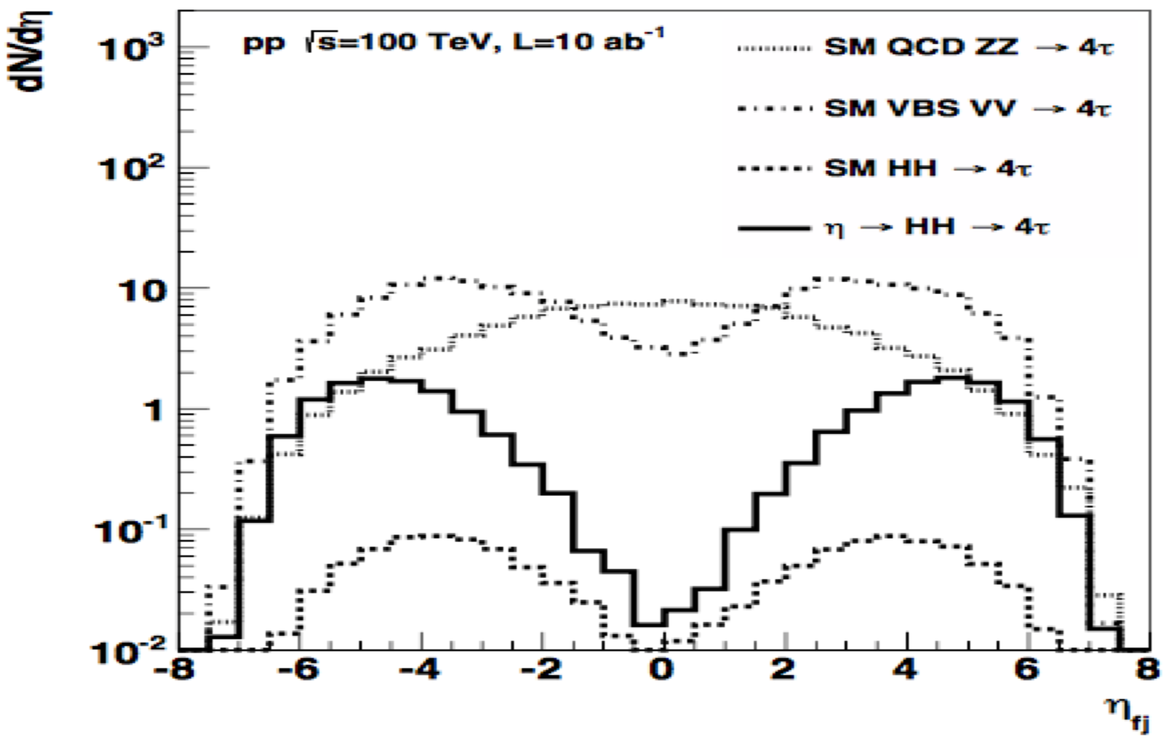

(a)The pseudo-rapidity distributions of the forward jets.

Forward Jet Coverage for Longitudinal VBS

$V_L V_L \to \eta \to HH$

AVK, S. Chekanov, M. Low

TABLE II. 5σ discovery mass reach for the $\eta \to HH \to 4\tau$ resonance, at a pp collider with $\sqrt{s} = 100$ TeV and $\mathcal{L} = 10\ \mathrm{ab}^{-1}$, for various cuts values on minimum p_T of the forward jets. The fractional width of the η resonance is set to $\Gamma/M = 20\%$.

$p_T^{\min}$ (GeV)	30	50	70	90	110
m_η (TeV)	3.53	2.90	2.35	1.92	1.56

- Lower p_T threshold on forward tagging jets is preferred
  - Reject pileup jets with good tracking in forward direction
  - Resolve overlapping pileup jets with higher granularity / spatial resolution (*a la* CMS high-granularity endcap calorimeter for HL-LHC)

Vector Boson Scattering

Double Higgs Boson Production in the 4τChannel from Resonances in Longitudinal Vector Boson Scattering at a 100 TeV Collider

AVK, S. Chekanov, M. Low
Phys.Rev. D91 (2015) 114018

TABLE III. 5σ discovery mass reach for the $\eta \to HH \to 4\tau$ resonance, at a pp collider with $\sqrt{s} = 100$ TeV and $\mathcal{L} = 10$ ab^{-1}, for various cuts values on the maximum rapidity (y) of the forward jets. The fractional width of the η resonance is set to $\Gamma/M = 20\%$.

$y^{\max}$	8	7	6	5	4
m_η (TeV)	2.9	2.9	2.81	2.42	1.75

Want jet rapidity coverage up to 6

Conclusions

- proton-proton colliders (at very high energy) provide unprecedented discovery potential in the diHiggs channel

- New territory explored with precision measurements and direct searches is strongly motivated for
  - Solving the mysteries associated with the Higgs boson and the Higgs self-coupling
  - Understanding the electroweak phase transition and discovering the conditions for electroweak baryogenesis
  - DiHiggs resonances accessible only via longitudinal vector boson scattering

- In the singlet scalar extension of the standard model, the parameter phase space enabling a strongly 1^{st} order electroweak phase transition is completely discoverable at a 100 TeV *pp* collider

Backup Slides

2. Option 2: Twin Solenoid + Dipoles

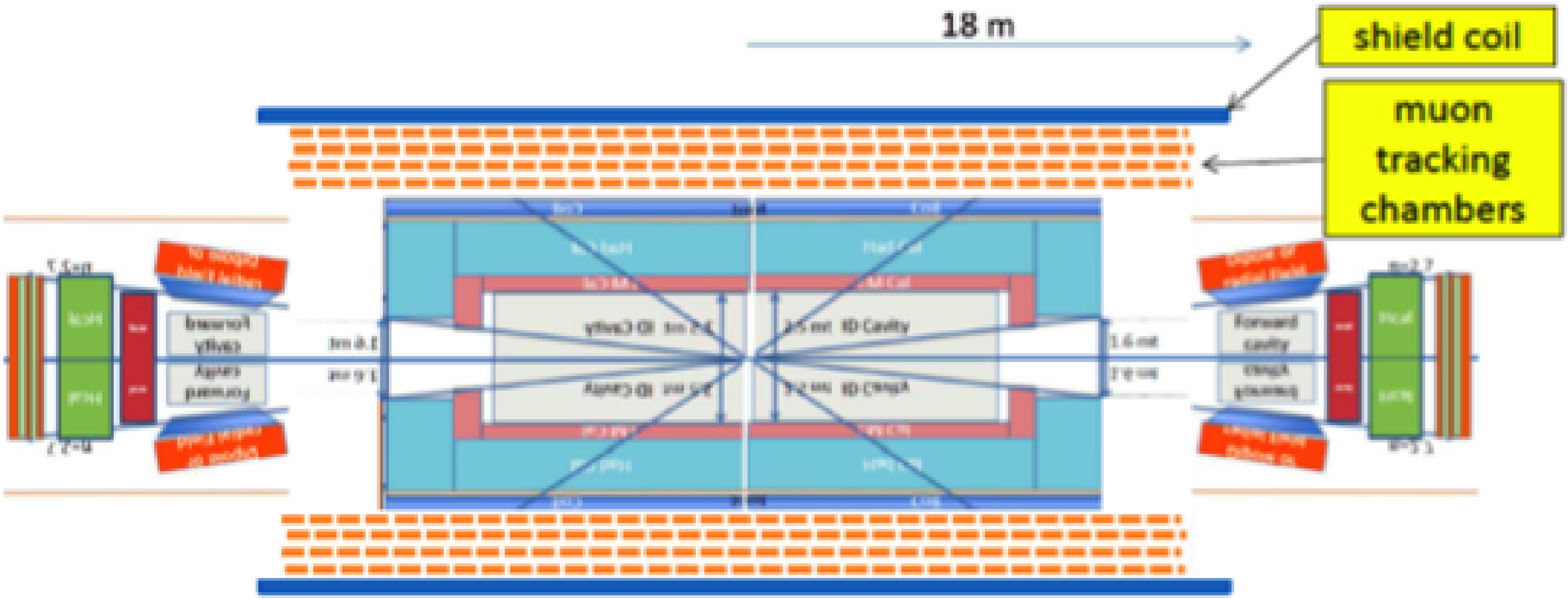

Twin Solenoid: a 6 T, 12 m dia x 23 m long main solenoid + an active shielding coil

Important advantages:

- ✓ **Nice Muon tracking space:** area with 2 to 3 T for muon tracking in 4 layers.
- ✓ **Very light:** 2 coils + structures, ≈ 5 kt, only ≈ 4% of the option with iron yoke!
- ✓ **Much smaller:** system outer diameter is significantly less than with iron .